

A Condition Monitoring System for Electric Vehicle Batteries Based on a Convolutional Neural Network Using Thermal Image

S.Senthilraj¹, N. R. Shanker²

¹ Research Scholar, Electronics and Communication Engineering,
PRIST University,
Thanjavur, Tamil Nadu, India
senthilrajvlsi@gmail.com

² Professor / Supervisor, Computer Science and Engineering,
Aalim Muhammed Salegh College of Engineering,
Chennai, Tamil Nadu, India
nr_phd@yahoo.in

Abstract— A new monitoring technique has been developed to evaluate the capacity and performance of Lithium-ion batteries by utilizing two convolutional neural networks (CNNs) models, Deep convolutional neural network (DnCNN) and CNN with BFGS quasi-Newton optimization. The system utilizes thermal images of lithium-ion batteries as input for training and testing. DnCNN model is utilised to accurately calculate battery capacity and performance, and the performance is evaluated using mean squared error (MSE) and PSNR. The CNN-based training method employs the BFGS quasi-Newton algorithm to measure battery capacity accurately by evaluating the mean squared error (MSE) and regression results. The proposed condition monitoring system using thermal imaging and CNN models, specifically the CNN- BFGS quasi-Newton algorithm model, can accurately detect battery capacity with an accuracy rate of 98.5%, compared to the DnCNN model with an accuracy rate of 96.7%. The proposed system can address the critical issue of battery capacity and degradation in EVs, providing a more sustainable and efficient alternative for real-time applications.

Keywords- Electric vehicle (EV); Deep Convolutional Neural Network (DnCNN); Convolutional Neural Network (CNN); BFGS Quasi-Newton method; Mean Square Error (MSE).

I. INTRODUCTION

An electric vehicle is a vehicle that uses one or more electric or traction motors to move. It can be powered by self-contained batteries or non-renewable sources, fuel cells or solar panels, but the latter is a more expensive option. Electric vehicles can be used for all types of transportation, including road and rail vehicles, watercraft, aircraft, and spacecraft.

The modern world requires advanced technology to address current and future challenges. In India, the primary challenge is the scarcity of fossil resources, with fuel prices continuing to rise daily and causing a significant amount of pollution. To combat this, we must shift towards electric vehicles generated by renewable energy sources such as wind and solar energy. Battery management systems are crucial for maintaining the safe and reliable operation of batteries, monitoring and controlling charging and discharging rates, charge level, health, life, and maximum capacity. Monitoring techniques like current, voltage, and ambient temperature are used to maintain battery's charge level.

Electric vehicles are crucial because they emit no harmful emissions and are energy-efficient. They require an

efficient battery management system to provide sufficient power to their numerous battery cells, with lithium-ion batteries being the most commonly used due to their merits and effectiveness. Typically, the estimated range of an electric vehicle's battery is 30 to 100 kWh or higher. Environmental issues due to gasoline vehicles and low fuel consumption have made the development of green, ecologically-friendly, and economical vehicles a critical goal for many countries.

Electric vehicles have comparable mileage and fuel economy to gasoline vehicles, with zero environmental emissions, high mileage, and low fuel consumption. Lithium-ion batteries are the de facto standard for automobile power batteries, with a high energy density, low self discharge rate, high open circuit voltage, and no memory effect. They have an optimal value of 113.8 MW, representing 54.7% of the total capacity of new energy storage projects worldwide. In conclusion, lithium-ion batteries appear to have a bright future in the realm of electric vehicles.

We categorize various charging and discharging tactics for plug-in electric vehicles in detail, identifying their differences in complexity, economics, power losses, ancillary services,

timing, and environmental impact. We provide recommendations and ratings for specific applications, helping researchers and developers choose the best option for their systems or test beds. This evaluation fills a void in the literature and assists in identifying potential candidates [1]

In this study, we analyze the battery management system (BMS) for rapidly exchanging battery packages in EV buses. We examine the BMS structure and function, as well as charging, maintenance, recombination, state of charge calibration, and parametric recognition during the exchanging process. This investigation is based on the unique features of this new battery exchange mode [2].

The improved loaded voltmeter test (ILVT) uses a stored function of battery voltage measurements with a fixed resistor load, allowing for specific charge values to be found without harming the electricity system. Haifa found no increase in errors when using the ILVT instead of the standard loaded voltmeter test for lead-acid batteries. The ILVT can also be applied to test other battery types [3].

A new battery management system has been proposed as a solution for electric vehicle battery issues. This system divides the battery in half for charging and discharging. Sustainable energy sources charge the vehicle while one half discharges, and vice versa. This eliminates external charging and the need for two distinct batteries. The design, analysis, advantages, and potential applications of this system are discussed, including resolving the electric vehicle's inclination problem [4].

We examine safe charging of electric vehicles from both grid-side and equipment-side perspectives, aiming to optimize the charging structure's design. With the growing popularity of electric vehicles, charging safety will become a priority, and this article proposes the best approach for safely charging electric vehicles in the power grid. The heat management process helps to regulate their interior temperature of the battery system, ensuring that charging and discharging occur within a safe temperature range. Our comprehensive solution effectively controls charging safety, minimizing potential hazards, and encouraging the widespread adoption of electric vehicles [5].

Electric vehicles (EVs) are increasingly replacing gasoline vehicles, contributing to the fight against global warming. The electric vehicle's energy storage system will be supported with lithium-ion battery banks, known for their high capacity and efficiency. However, to avoid damaging the battery, a control model must protect it from over- or undercharging. This study employs Simulink software to assess the efficiency of a Li-ion battery energy management approach over electric vehicles, which includes a bidirectional flyback DC-DC converter and an intelligent charge control

algorithm to maintain a safe cell voltage range (3.73 V - 3.87 V) through regulated PWM signals [6].

For hybrid and electric vehicles, battery management is critical to optimize their energy management and extend the battery's life by monitoring SOC and SOH. This paper presents research on intelligent state of charge prediction based on a lumped battery model utilizing an extended Kalman filter. The Kalman filter has been extended to account for battery ageing effects. The simplified models are implementable on a digital signal processor, and the charge observer's real-time status has been evaluated on a lithium-ion cell under different operating situations. [7].

Developing an accurate method for predicting a battery's remaining capacity is crucial for electric vehicle experts. However, various battery types or models require different prediction models, and expert advice may not be universal. To address this issue, this article focuses on iron phosphate Li-ion batteries and proposes a neural network approach for constructing a prediction model based on charge-discharge performance tests. The model's validity is tested using real-world data [8].

This article compares the characteristics of lithium-ion and lead-acid batteries, specifically the charging and discharging processes using adjustable current or pulse current. The charging behavior of these batteries begins with constant current followed by constant voltage. The system utilized in this study measures voltage, current, and temperature and is equipped with the ability to log data to a personal computer [9].

To understand a lithium battery's properties, its impedance in a single state of charge (SoC) is important. While some analyzers can measure this impedance, doing so across multiple SoCs is time-consuming. We propose a new method to compute impedance across different SoCs while changing them. Our method generates reliable results even with non-linear behavior. The data is validated by comparing it with impedance data taken from a no-load cell at different SoCs [10].

The pursuit of efficient battery systems creates challenges for engineers and scientists in developing cost-effective mobile energy storage. Accurate battery behavior modeling is necessary for providing a suitable battery for a mobile device. Precision measurements are needed for constructing accurate models. This article presents and evaluates a quick, highly accurate, and fully configurable battery measurement device. A current source capable of delivering and sinking currents of up to 32 A over a frequency range of DC to 20 kHz is included, as are a high level voltage, current, and temperature meters. [11].

Typically, a battery is the energy storage medium of choice for mobile applications, and a suitable battery model is

required for system component design and optimization through simulation. Parameter determination needs data from measurement. This article describes a prototype measurement system capable of collecting data from batteries with capacities ranging from certain mAh for connected devices to multiple hundred Ah for electric automobiles and hybrid electric vehicles, facilitating testing and parameter identification [12].

The article examines the charging and discharging characteristics, and also the operation, of lithium-ion batteries, particularly LixC6 and LiyMn2O4 batteries. Simulating the electrochemical processes of these batteries with an analytical model gives a dynamic model that represents the temporary state of the battery result. The study investigates the battery's voltage, current, temperature, state of charge, and charging and discharging properties. The model can be used to accurately control battery charging and discharging strategies and measure state of charge (SOC) and part of laboratory setup for modeling electrochemical energy storage system of electric or hybrid vehicles [13].

Battery monitoring industry faces the challenge of assessing and predicting battery performance. Thermal imaging is a nondestructive evaluation technique that provides vital information about a battery's electrochemical performance due to its impact on internal chemistry. In this research, a refined approach linking thermal imaging to internal battery reactions is proposed to define early failure detection descriptors. This method has been experimentally proven using lead-acid batteries, highlighting the challenges of operando battery thermal imaging and the need for future iterative design advancements [14].

Lithium-ion batteries are preferred for electric vehicles (EVs) due to their eco-friendliness and various advantages. However, their charging and discharging behavior is influenced by the charging current intensity, which varies among manufacturers and cells. This study examines charge and discharge behavior of cylindrical cells under low voltage and suggests ways to avoid undercharging in EVs using constant current and voltage measurements in Chroma 17011 equipment. [15].

II. INFERENCE FROM THE LITERATURE SURVEY

In this research, the focus is on monitoring the condition of lithium-ion batteries through utilizing neural networks. The aim is to reduce the time and resources required for experiments while accurately detecting the battery's capacity. Two training methods, DnCNN and CNN with BFGS quasi-Newton optimization, are introduced as part of a new battery monitoring system. The system utilizes thermal images of the battery to measure the performance of the training. The proposed method results are effective in

accurately calculating battery capacity while also reducing the time and resources required for experimentation. This has implications for improving the efficiency and long-term reliability of lithium-ion batteries in several types of applications.

III. METHODOLOGY

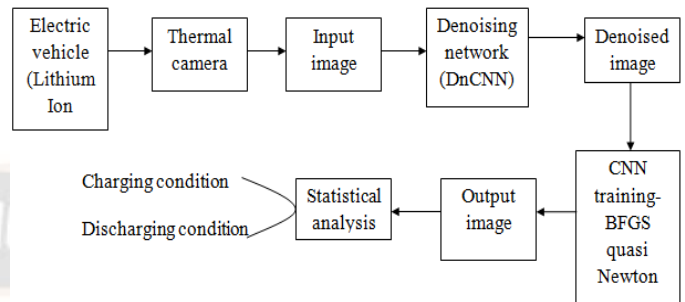


Figure 1 Block diagram of the proposed techniques

Li-ion batteries are made up of four major components: a cathode, an anode, an electrolyte, and a separator, each of which is essential to the battery's accurate operation. Without any of these components, the battery's performance will be hindered.

In contrast to traditional batteries, lithium-ion batteries offer several advantages such as faster charging, longer lifespan, and better energy density, enabling them to last longer in a smaller container. Lithium iron phosphate (LFP) is a cathode chemistry that is inherently safer than other alternatives but has intellectual property restrictions. It has a high power density, making it an ideal choice for electric tools and e-buses and a feasible option for electric vehicles.

Li-ion batteries have a positive electrode that contains a lithium compound, which undergoes intercalation, and a negative electrode usually composed of graphite. These batteries have a high energy density, exhibit minimal memory effect (lithium-ion polymer cells being an exception), and possess a low self-discharge rate.

Battery Specification:

| | |
|------------------------|----------|
| Voltage | 51.8 V |
| Current | 20 Ah |
| Weight | 10.5 Kg |
| Each Cell Max Voltage | 4 V |
| Each Cell Min Voltage | 3.7 V |
| Each Cell Power Rating | 37.00 Wh |
| Total Cells | 28 Cells |

Charger Specification:

| | |
|----------------|----------------------|
| Model | NG1 Battery Charger |
| Input Voltage | 230V AC, 6A, 50-60Hz |
| Output Voltage | 50.4V DC, 12A |



Figure 2. Battery charging setup

To charge individual battery cells, the RPS positive is linked directly to the positive terminal, and the RPS negative is connected to the negative terminal. To charge the entire battery cell, it is recommended to maintain a current between 1A to 1.5A at RPS. For charging a single cell, the current in RPS should be limited to 1A, and the voltage must not exceed 1.5V.



Figure 3. Battery Discharging set up

To measure current in amperes, the positive terminal of the ammeter (or multimeter in ampere mode) connects directly to the battery positive end. The ammeter negative terminal is connected to 2000 W load. The load's opposite end is linked to the negative terminal of the battery through a 20-amp fuse.

A. Convolutional Neural Network (Cnn)

A convolutional neural network, a type of feedforward neural network that performs convolution, includes a depth structure. It is widely utilized in various domains, such as natural language processing and computer vision. The CNN consists of three layers: input, hidden, and output. A schematic design of a convolutional neural network illustrated in Figure 4. The CNN hidden layer comprises three elements: weighted convolution kernel process in the convolutional layer, a filtering process in the pooling layer, and a connection process in the tiled layer, which is also known as a fully connected layer.

1) *Convolutional Layer*: The convolutional layer acquires data from the input data using a predefined

convolution kernel. This kernel is defined by three essential parameters: step size, kernel size and padding, which collectively evaluate the produced feature map dimension of the convolutional layer. An activation function is commonly applied in the convolutional layer to express complex input properties, and the ReLU function is often used in CNN. Even though the activation function is applied following the convolution kernel, it is not fixed. Additionally, there are numerous activation functions that are not always carried out in the same spot.

2) *Pooling Layer*: After the convolutional layer completed the input, a feature map is generated, and the pooling layer is then utilized to select features and filter data on this map. Similar to the convolution kernel, the pooling layer has its own parameters for step size, pooling size and filling control. In contrast to the convolution kernel, which is used for measured sum, the pooling layer modifies these parameters to maximize or normalize feature values. In addition, the pooling layer can decrease the amount of nodes in the fully linked layer, so preventing overfitting.

3) *Fully Connected Layer*: The CNN fully connected layer resembles the hidden layer of a BP neural network in structure and function. Its purpose is to produce the desired output by performing a series of nonlinear combinations on the extracted features derived from the input sample of convolutional pooling.

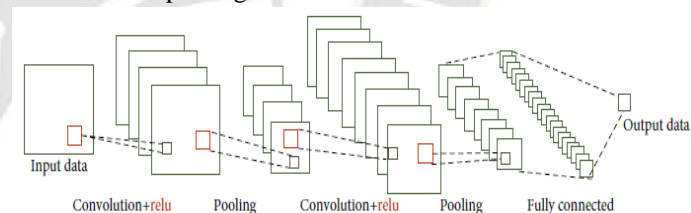


Figure 4: Structure of CNN

B. Learning Deep Cnn for Image Denoising

Due to its superior denoising performance, discriminative model learning for image denoising has recently garnered substantial attention. We take a step ahead by examining the formation of feed-forward denoising convolutional neural networks (DnCNNs) and integrating advancements in deep architecture, learning algorithms, and regularisation methods into picture denoising.

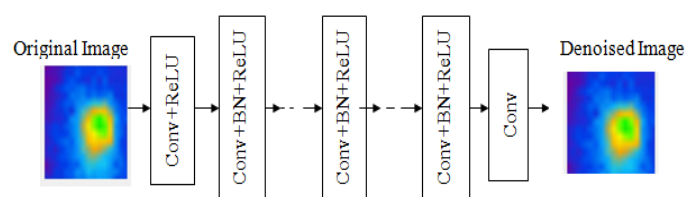


Figure 5. The architecture of DnCNN

The DnCNN architecture is illustrated in Fig. 5. It accepts noisy input $y = x + v$, where v is noise and x is clean image. Unlike training residual mapping $R(y) = v$, DnCNN trains residual mapping $R(y) = v$ before computes $x = y - R(y)$. Size of fixed convolutional filters is 3×3 , and resolution of the convolutional layer with depth d is $(2d + 1) \times (2d + 1)$, following the principle. Raising network depth increases utilisation of metadata in a larger image region but also increases the computational load, necessitating a trade-off between performance and reliability in architectural design. DnCNN has an accessible field level of 35×35 for Gaussian denoising with a depth of 17 at a particular noise level. As illustrated in Fig. 5, a DnCNN with depth D is capable of utilizing the following three types of layers:

- (i) Conv + ReLU: The first layer uses 64 filters of dimension $3 \times 3 \times c$ to generate 64 feature maps, which are then subsequent by rectified linear units (ReLU, $\max(0, \cdot)$).
- (ii) Conv + BN + ReLU: layers $2 \sim (D - 1)$ employ 64 filters of dimension $3 \times 3 \times 64$, with batch normalisation applied to both ReLU and convolution.
- (iii) Conv: the final layer reconstructs the denoising output using $3 \times 3 \times 64$ c filters.

To evaluate the performance of DnCNN in denoising thermal images of Lithium-ion batteries, two commonly used metrics are Peak Signal-to-Noise Ratio (PSNR) and Mean Squared Error (MSE).

MSE measure average squared difference among estimated denoised image and original image. It can be calculated using the following equation:

$$MSE = \frac{1}{m \cdot n} \sum_{i=0}^{m-1} \sum_{j=0}^{n-1} [I(i, j) - K(i, j)]^2 \quad (1)$$

where m and n are dimensions of image, $I(i, j)$ is pixel value of original image at position (i, j) , and $K(i, j)$ is corresponding pixel value at position (i, j) of denoised image.

PSNR is the ratio among the maximum potential power of an image and noise power that reduces its representational accuracy. It's expressed in decibels (dB) and can be calculated using the following equation:

$$PSNR = 20 * \log_{10} \left(\frac{MAX_I}{\sqrt{MSE}} \right) \quad (2)$$

Where MAX_I the maximum potential value of pixel intensity and MSE is mean squared error between original and denoised images.

MSE and PSNR are two important metrics that can be used to evaluate the performance of DnCNN in denoising thermal images of Lithium-ion batteries. By minimizing the MSE and maximizing the PSNR, DnCNN can achieve better denoising performance, which can ultimately lead to more accurate analysis and prediction of the battery's thermal behavior.

C. Training Process: Bfgs Quasi Newton Techniques

Quasi-Newton techniques are well-known for processing problems involving unconstrained optimization. On the other side, Broyden, Fletcher, Goldfarb, and Shanno proposed a new optimising formula, named BFGS, that has now received wide utilisation and gone numerous changes.

In summary, the section describes unconstrained optimization problems:

$$\min_{x \in R^n} f(x) \quad (3)$$

where R_n denotes n -dimensional Euclidean space and $f: R^n \rightarrow R$ denotes continuous twice differentiable space. For equation (1), the gradient and Hessian are represented by the letters g and G , respectively. To present the modified BFGS equation, the step-vectors S_k and y_k are summarized as follows:

$$\begin{aligned} S_k &= x_{k+1} - x_k \\ y_k &= g(x_{k+1}) - g(x_k) \\ &= g_{k+1} - g_k \end{aligned} \quad (4)$$

Concerning quasi-Newton approaches, we will depend on the BFGS method, which has been demonstrated is the most powerful of all quasi-Newton methods. Thus, if B_k is defined as a close approximation to Hessian G at x_k , the iterative equation for BFGS is as follows:

$$B_{k+1} = B_k - \frac{B_k s_k s_k^T B_k}{s_k^T B_k s_k} + \frac{y_k y_k^T}{s_k^T y_k} \quad (5)$$

Additionally, it is generally known that (5) generates the matrix B_{k+1} in fulfil the secant equation.

$$B_{k+1} s_k = y_k \quad (6)$$

It might be thought of as an approximation to Newton's theory. Realize that the secant equation can be satisfied only if

$$s_k^T y_k > 0 \quad (7)$$

It is referred to as the curved condition. Additionally, if (7) holds, the BFGS updating matrix (5) will be positive definite.

Iterative technique is utilised to analyse unconstrained optimization issues in order to obtain the function's minimum value where gradient is 0. As a result, iterative solution for quasi-Newton method is specified.

$$x_{k+1} = x_k + a_k d_k \quad (8)$$

where a_k and d_k represent step size and direction of search, appropriately. Step size has to be positive in order to $f(x)$ is significantly reduced. A line search's success is based on effective selections of both direction of the search d_k and the step size a_k . There are numerous algorithms for computing the step size, which are classified as inexact and exact line searches.

Possibly the ideal solution for exact line search equation, given as $a_k = \arg \min (f(x_k + a_k d_k))$ $a > 0$ but identifying this value is generally more cost. Normally, it needs an infinite number of calculations for target function f and gradient g . Some equations for the inexact line search have been proposed previously. The Armijo line search is the most efficient and simple of the numerous well-known inexact line search algorithms used in computer calculations. Additionally, it is simple to apply in coding such as Matlab and Fortran. The following description of the Armijo line search is:

Provided $s > 0$, $\lambda \in (0,1)$ $\sigma \in (0,1)$ and $a_i = \max\{s, s\lambda, s\lambda^2, \dots\}$ as if

$$f(x_k) - f(x_k + a_k d_k) \geq -\sigma a_k g_k^T d_k \quad (9)$$

$k = 0, 1, 2, 3, \dots$ The reduction in f has to be inversely proportional to both step size and directional derivative $g_k^T d_k$. The search directions are essential to improving value of f , that reduces with direction. Additionally, quasi-Newtonian techniques frequently have the following search direction:

$$d_k = -B_k^{-1} g_k \quad (10)$$

where B_k is a synchronous and nonsingular estimation matrix to the Hessian matrix (5). An identity matrix is used to select the initial matrix B_0 , and is then modified using an update equation. Where d_1 is denoted in equation (8) and B_k is significant positive, and obtain $d_k^T = -g_k^T B_k^{-1} g_k < 0$, indicating that dk is a direction of descent. As a result, the

methodology for an iteration approach of standard BFGS is as follows:

Algorithm

Step1: Given a starting location x_0 and a value for B_0 equal to I_n . Select values for s, β , and σ

Step2: Cancel if $\|g(x_{k+1})\| < 10^{-6}$

Step3: Compute the direction of the search by (8).

Step4: compute the step size α by (7).

Step5: calculate the variation $s_k = x_{k+1} - x_k$ and $y_k = g_{k+1} - g_k$

Step6: modify B_k by (3) to acquired B_{k+1}

Step7: make k equal to $k + 1$ and proceed to Step 1

IV. RESULTS AND DISCUSSION

To evaluate the proposed system's performance, charging and discharging properties of lithium battery tested in normal temperature condition are manually determined using a multimeter attached to the battery terminals. The time taken to charge the battery is 4 hours, where the voltage and current variation are measured for each 15 minutes interval as shown in the table1. To reach 100% capacity of the battery, the voltage starts from 45.7v to 55.8V and the current starts from 2.4A to 4.2A respectively. The 9 hours taken to discharge the battery at load of 2000W, where the voltage and current variations are measured for each 30 minutes interval as shown in the table2. To obtain battery capacity low, the voltage starts gradually reduce from 55.8V to 44V and the current from 2.01A to 1.59A respectively. On lithium-ion battery original dataset, the developed CNN-based capacity estimating algorithm Deep convolutional neural network (DnCNN) and CNN with BFGS quasi-Newton optimization is applied. The maximum number of training epochs is defined to 50 during the training phase, and the step size is defined to 100 samples. The battery's health is monitored twice: while charging and discharging.

TABLE I. THE VOLTAGE AND CURRENT ARE MEASURED MANUALLY DURING CHARGING STATE AND DISCHARGING STATE

| S.N | CHARGING STATE | | | DISCHARGING STATE | | |
|-----|----------------|-------|-------|-------------------|-------|-------|
| | TIME | MSE | PSNR | TIME | MSE | PSNR |
| 1 | 01:30 | 55.62 | 30.49 | 10:00 | 59.66 | 30.57 |
| 2 | 01:45 | 49.36 | 30.67 | 11:00 | 58.93 | 30.89 |
| 3 | 02:00 | 55.34 | 30.41 | 11:30 | 62.20 | 30.46 |
| 4 | 02:15 | 53.67 | 30.46 | 12:00 | 54.05 | 30.99 |
| 5 | 02:30 | 53.72 | 30.43 | 12:30 | 57.22 | 30.85 |
| 6 | 02:45 | 55.34 | 30.48 | 01:00 | 54.89 | 30.84 |
| 7 | 03:00 | 57.11 | 30.38 | 01:30 | 58.74 | 31.09 |
| 8 | 03:15 | 60.12 | 30.39 | 02:00 | 56.41 | 31.49 |
| 9 | 03:30 | 56.17 | 31.08 | 02:30 | 60.20 | 30.49 |
| 10 | 03:45 | 57.92 | 30.62 | 03:00 | 55.71 | 31.69 |

| | | | | | | | | | | | | | |
|----|-------|-------|-------|-------|-------|-------|----|-------|------|-----|-------|------|------|
| 11 | 04:00 | 56.16 | 30.54 | 03:30 | 62.79 | 30.27 | 14 | 04:45 | 53.9 | 4.2 | 05:00 | 49.5 | 1.77 |
| 12 | 04:15 | 50.97 | 30.89 | 04:00 | 62.94 | 30.21 | 15 | 05:00 | 54.4 | 4.2 | 05:30 | 49.1 | 1.75 |
| 13 | 04:30 | 52.55 | 32.04 | 04:30 | 61.63 | 30.48 | 16 | 05:15 | 55.1 | 4.2 | 06:00 | 47.4 | 1.69 |
| 14 | 04:45 | 52.49 | 32.02 | 05:00 | 62.20 | 30.38 | 17 | 05:30 | 55.8 | 4.2 | 06:30 | 44 | 1.59 |
| 15 | 05:00 | 54.12 | 32.13 | 05:30 | 62.74 | 30.23 | | | | | | | |
| 16 | 05:15 | 55.48 | 32.31 | 06:00 | 59.40 | 30.31 | | | | | | | |
| 17 | 05:30 | 53.23 | 31.81 | 06:30 | 59.32 | 30.92 | | | | | | | |

PSNR (Peak Signal-to-Noise Ratio) and MSE (Mean Squared Error) are commonly used metrics to evaluate the quality of reconstructed images compared to the original data. In the context of charging and discharging states of lithium-ion batteries, these metrics can be calculated using a Deep Neural Network (DNN) such as DnCNN (Denoising Convolutional Neural Network). To calculate MSE, the DNN is trained to estimate the charging or discharging state of a lithium-ion battery from a given input image. The MSE is calculated as mentioned in the equation 1. A lower MSE value indicates better performance of the DNN in estimating the battery state.

PSNR is another metric that measures the quality of reconstructed image. It is calculated as the ratio between the maximum possible and the noise power that influences the representation's accuracy. In lithium-ion battery charging and discharging states, PSNR is used to evaluate the quality of the estimated state by comparing it to the original state. Higher PSNR values indicate better quality of reconstructed image. Overall, PSNR and MSE are useful to evaluate the efficiency of DnCNN in estimating the charging and discharging states of lithium-ion batteries. By optimizing these metrics during the training process, the DNN can be better tailored to accurately determine the battery's health, which is important for monitoring and controlling its behaviour with an accuracy rate of 96.7%.

TABLE II: MSE AND PSNR ARE CALCULATED FOR CHARGING STATE AND DISCHARGING STATE USING DNCNN

| CHARGING PROCESS | | | | DISCHARGING STATE | | |
|------------------|-------|--------|-------|-------------------|--------|--------|
| S.N | TIME | VOLTA | CURRE | TIME | VOLTA | CURRE |
| O | | GE (V) | NT(A) | | GE (V) | NT (A) |
| 1 | 01:30 | 45.7 | 2.4 | 10:00 | 55.8 | 2.01 |
| 2 | 01:45 | 47.1 | 3.1 | 11:00 | 55.0 | 1.94 |
| 3 | 02:00 | 48.4 | 4.2 | 11:30 | 53.5 | 1.92 |
| 4 | 02:15 | 49.0 | 4.2 | 12:00 | 52.9 | 1.90 |
| 5 | 02:30 | 50.5 | 4.2 | 12:30 | 52.4 | 1.88 |
| 6 | 02:45 | 50.9 | 4.2 | 01:00 | 52.1 | 1.87 |
| 7 | 03:00 | 51.2 | 4.2 | 01:30 | 51.7 | 1.85 |
| 8 | 03:15 | 51.7 | 4.2 | 02:00 | 51.3 | 1.84 |
| 9 | 03:30 | 52.0 | 4.2 | 02:30 | 51.0 | 1.82 |
| 10 | 03:45 | 52.2 | 4.2 | 03:00 | 50.8 | 1.81 |
| 11 | 04:00 | 52.6 | 4.2 | 03:30 | 50.4 | 1.81 |
| 12 | 04:15 | 53.0 | 4.2 | 04:00 | 50.3 | 1.80 |
| 13 | 04:30 | 53.3 | 4.2 | 04:30 | 49.7 | 1.78 |

A. Performance Analysis of BFGS Quasi-Newton Optimization for Charging State

CNN is trained on thermal images of the battery, which are used to detect any abnormalities or defects that may be present. The BFGS Quasi-Newton Optimization algorithm is used to optimize the CNN's performance and improve its accuracy. The process begins with the acquisition of thermal images of the battery. These images are then preprocessed and normalized to ensure that they are suitable for input into the CNN. The CNN consists of multiple layers of interconnected nodes or neurons, which are responsible for processing the input data and producing the desired output.

The CNN is trained using a dataset of labeled thermal images, which have been annotated with information about the battery's condition. The network learns to map the thermal images to their corresponding labels using a process known as supervised learning. The BFGS Quasi-Newton Optimization algorithm is utilised to optimize network's performance by adjusting its parameters to reduce error among predicted and actual labels. Once network has been trained, it can be used to analyze new thermal images of the battery and detect any abnormalities or defects that may be present. The output of the CNN can be visualized using a heatmap, which highlights areas of the battery that are experiencing higher temperatures or abnormal behavior.

To examine the performance of CNN models with varying numbers of convolutional layers under charging conditions, an identical training and testing approach is applied to all tests. The training and testing processes for each CNN configuration are run multiple times, and an average MSE and regression value are given in Table 3. The figure 7 demonstrates the denoised image for DnCNN models. Figure 8 shows the structure of training BFGS Quasi-Newton Neural Network for charging state with convolutional layers and the parameters involved in each configuration.

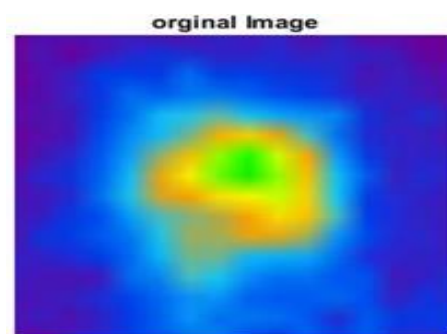


Figure 6: Original image of charging state

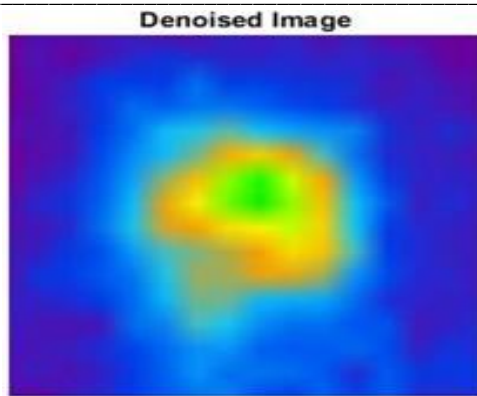


Figure 7: Denoised image of charging state

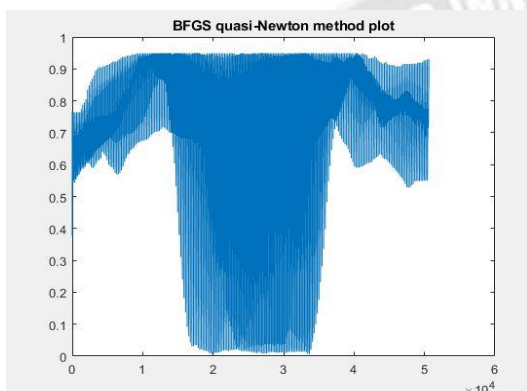


Figure 8: The plot of training BFGS Quasi-Newton for charging state.

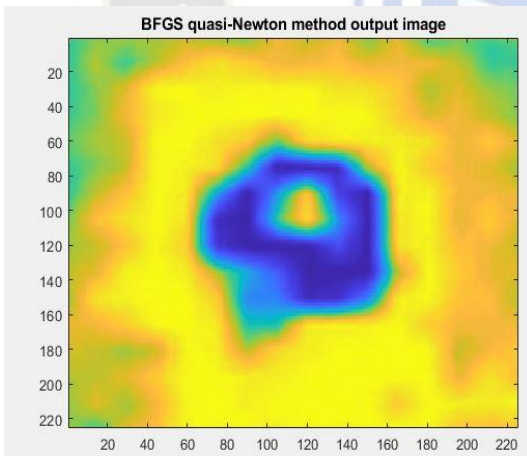


Figure 9: The output image of training BFGS Quasi-Newton for charging state

The figure 8 represents to monitor the convergence of the optimization process over time. The convergence of the algorithm could be demonstrated by plotting the value of the cost function throughout the period of training. The cost function represents the difference among predicted outputs in neural network and true outputs for a given set of input data. The aim of the optimization process is to reduce the cost function, which indicates that the neural network is making accurate predictions. In a typical plot of the cost function over

time, the x-axis represents number of iterations or epochs, and y-axis represents value of cost function. As optimization algorithm progresses, value of cost function should decrease, indicating that the neural network is making more accurate predictions.

If the plot shows that value of cost function is reducing but is oscillating around a minimum, this could indicate that the learning rate is too high. In contrast, if the plot shows that value of cost function is not reducing over time, this could indicate that the learning rate is too low or that the neural network architecture needs to be adjusted.

Figure 9 represents the output plots image is to calculate the output images quality produced by trained neural network and also useful in identifying areas of concern in the battery and can guide improvements to the model's performance. Visual inspection of the output images can also provide valuable insights into the performance of the neural network. Output image commonly used to shows the change in temperature over time and can help identify areas where the battery is heating up or cooling down too quickly. A well-trained model will accurately identify these areas and provide a clear visualization of the temperature changes over time.

The network was initially trained using 50% of the data set and afterwards validated and tested with the remaining 50%. The starting weights were chosen by possibility, while the sizes of the hidden layers were measured through trial and error. An error target was specified as $MSE = 1$, and the neural network was approved if its MSE was equal to or below an error target.

CNN was trained using input parameters as current, voltage, and time to anticipate battery's natural decline over a 50-cycle period. The CNN training acquired an MSE of roughly 0.010056×10^{-6} and was typically considered satisfactory as presented in Figure 10. As represented in figures, the most amount of training epochs permitted in network is 50 because of limitations determined by specific validation tests. When network level is reached, the network is unable to train. This is a better value because it indicates the network is highly specialized in test sets, hence reducing overfitting (a phenomena that occurs in training set during a network becomes masters). After the training of the network was complete, the weights were documented so the actual network could assess the charge/discharge cycles depending on the inputs.

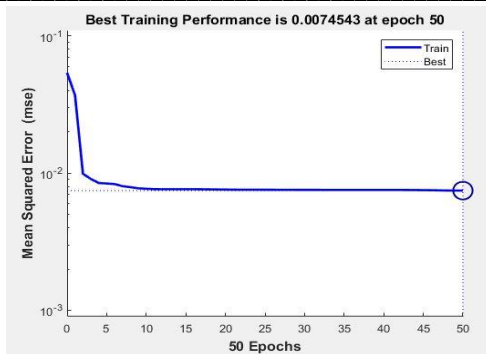


Figure 10. Best training performance at charging state

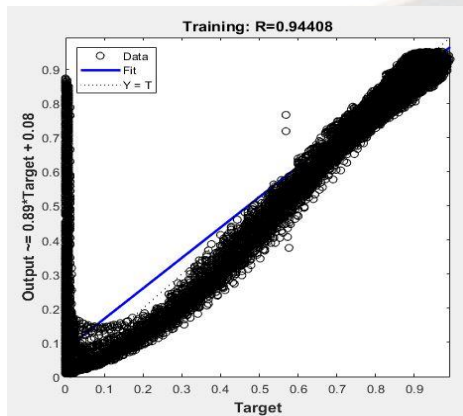


Figure 11: Regression analysis at charging state

TABLE 3. THE BEST TRAINING PERFORMANCE AND REGRESSION VALUE ARE MEASURED WITH DIFFERENT IMAGES DURING CHARGING STATES.

| CHARGING STATE – CNN TRAINING BFGS QUASI NEWTON METHOD | | |
|--|---------------------------------|------------|
| S. NO | BEST TRAINING PERFORMANCE (MSE) | REGRESSION |
| 1 | 0.0074543 | 0.94408 |
| 2 | 0.0095009 | 0.93582 |
| 3 | 0.0085957 | 0.93129 |
| 4 | 0.006028 | 0.94698 |
| 5 | 0.0055972 | 0.95112 |
| 6 | 0.0061224 | 0.95789 |
| 7 | 0.010056 | 0.96574 |
| 8 | 0.0080408 | 0.96784 |
| 9 | 0.0070078 | 0.97089 |
| 10 | 0.021053 | 0.86899 |
| 11 | 0.016238 | 0.77777 |
| 12 | 0.017789 | 0.95884 |
| 13 | 0.018129 | 0.87838 |
| 14 | 0.019473 | 0.85739 |
| 15 | 0.020384 | 0.84032 |
| 16 | 0.021784 | 0.81039 |
| 17 | 0.021307 | 0.79797 |

We defined 100% of the battery capacity performance during charging state; the battery in normal state gives the MSE value as 0.005×10^{-6} to 0.021×10^{-6} . Also the regression value will be in the range of 0.77 to 0.99. if, the performance analysis differ in the ranges as low and high, then the battery is in warning and abnormal state.

B. Performance Analysis of BFGS Quasi-Newton Optimization for Discharging State

As we discussed above the output of the CNN models perform in the above charging state will function as same in the discharging state. The training and testing methods are performed multiple times across every CNN configuration, and table 4 summarizes the average MSE and regression value. The figure 13 represents DnCNN models denoised image. Figure 16 shows the structure of training BFGS Quasi-Newton Neural Network for charging state with convolutional layers and the parameters involved in each configuration. When the discharging state is active, the battery temperature declines slowly as the cyclical changes.

We defined 100% of the battery capacity performance during discharging state of Lithium-ion batteries; thermal imaging can provide valuable information about the battery's internal temperature distribution during the discharging state. By analyzing the thermal images, it is possible to detect hotspots that may indicate potential safety hazards, as well as areas of the battery that may be operating at suboptimal temperatures. To analyze the performance of MSE and regression value for thermal images of Lithium-ion batteries in various states of discharge, with corresponding temperature measurements for each image. The performance of the CNN model can be calculated using a variety of measures, like MSE and regression value. Multiple measures, like the MSE and regression value, can be used to evaluate the performance of the CNN model. The MSE represents the average squared variation among the expected and actual temperature readings, while regression value is a measure of how well the predicted temperature values match the actual temperature values.

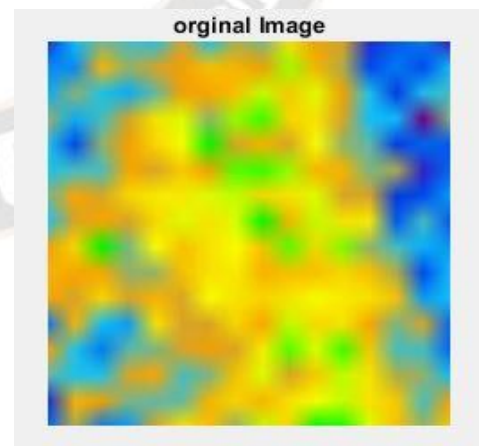


Figure 12: Original image of discharging state

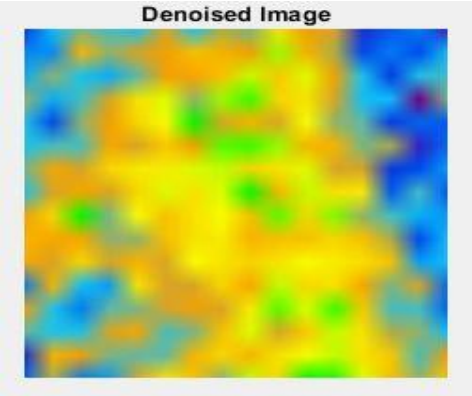


Figure 13: Denoised image of discharging state.

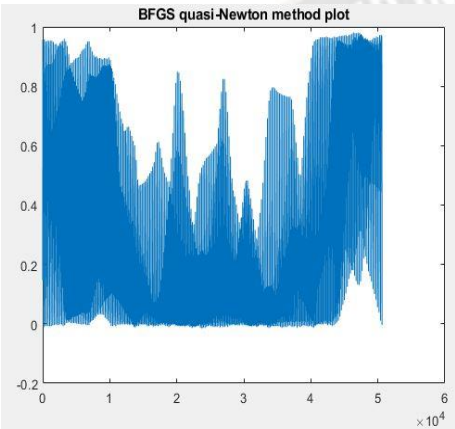


Figure 14: The plot of training BFGS Quasi-Newton for discharging state

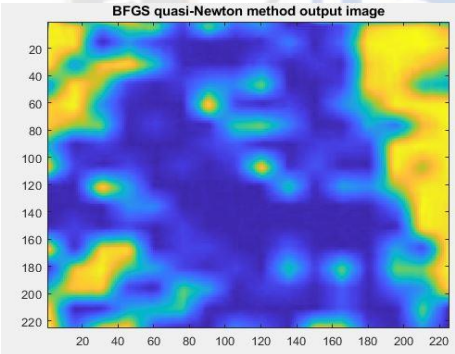


Figure 15: The output image of training BFGS Quasi-Newton for discharging state.

The battery in normal state gives the MSE value as 0.003×10^{-6} to 0.011×10^{-6} . Also the regression value will be in the range of 0.85 to 0.95. If, the performance analyses differ in the ranges as low and high, then the battery is in warning and abnormal state. By analyzing the performance for thermal images of Lithium-ion batteries during discharging state using CNN-BFGS Quasi-Newton optimization, it develops more accurate and reliable battery management systems.

Overall, a condition monitoring system using thermal imaging and CNN models, specifically the CNN- BFGS quasi-

Newton algorithm model, can accurately detect battery capacity with an accuracy rate of 98.5%.

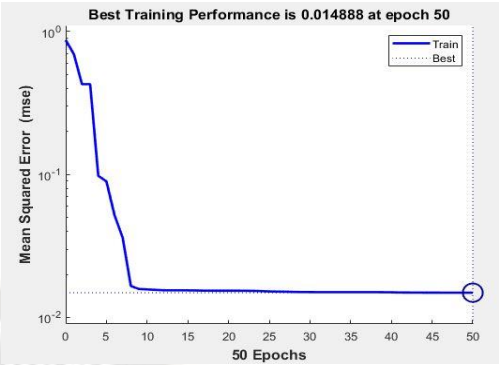


Figure 16: CNN training performance at discharging state

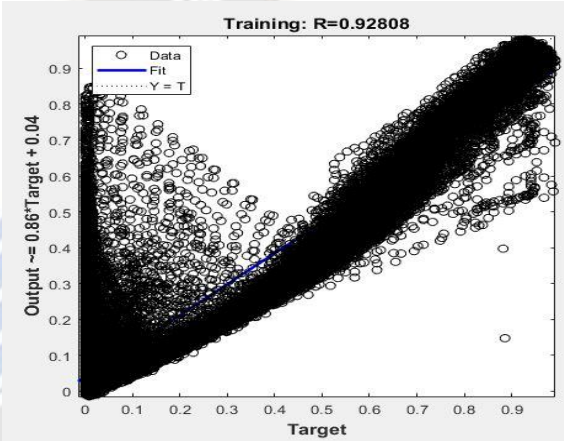


Figure 17: CNN training regression analysis at discharging state

Table 4. The best training performance and regression value are measured with different images during charging states.

| DISCHARGING STATE – CNN TRAINING BFGS QUASI NEWTON METHOD | | |
|---|---------------------------------|------------|
| S. NO | BEST TRAINING PERFORMANCE (MSE) | REGRESSION |
| 1 | 0.0086272 | 0.95923 |
| 2 | 0.030496 | 0.96725 |
| 3 | 0.0071346 | 0.97673 |
| 4 | 0.0042848 | 0.97886 |
| 5 | 0.0091669 | 0.96666 |
| 6 | 0.014888 | 0.92808 |
| 7 | 0.0081904 | 0.95780 |
| 8 | 0.014418 | 0.85124 |
| 9 | 0.006269 | 0.96038 |
| 10 | 0.0033074 | 0.97765 |
| 11 | 0.007909 | 0.95514 |
| 12 | 0.0079802 | 0.95336 |
| 13 | 0.0075384 | 0.94638 |
| 14 | 0.00724843 | 0.94939 |
| 15 | 0.00601276 | 0.92394 |
| 16 | 0.0060451 | 0.95669 |
| 17 | 0.0092979 | 0.93368 |

V. CONCLUSION

The use of thermal imaging to analyze Lithium-ion batteries has become increasingly important due to its ability to provide valuable information about the internal temperature distribution of the battery during operation. To further improve the accuracy and reliability of battery management systems, various image processing techniques have been developed, including DnCNN and CNN-BFGS Quasi-Newton Optimization. DnCNN is a deep learning algorithm that can be used to denoise thermal images and improve temperature measurements accuracy. Algorithm has been shown to be effective in reducing noise in thermal images and improving the quality of temperature measurements. In addition, CNN BFGS Quasi-Newton Optimization is a powerful optimization algorithm that can be used to train CNN models to predict temperature distributions of Lithium-ion batteries based on thermal images. This technique can improve the accuracy and reliability of temperature predictions, making it possible to detect potential safety hazards and areas of suboptimal performance. Overall, the use of DnCNN and CNN BFGS Quasi-Newton Optimization for analyzing thermal images of Lithium-ion batteries during operation can significantly enhance battery management systems' accuracy and reliability. The CNN- BFGS quasi-Newton algorithm model, can accurately detect battery capacity with an accuracy rate of 98.5%, compared to the DnCNN model with an accuracy rate of 96.7%. This has a major effect on the protection, efficiency, and lifespan of Lithium-ion batteries, which are crucial components in numerous applications, such as electric vehicles, portable electronics, and renewable energy systems. Therefore, further research in this area can lead to more efficient and reliable battery management systems that can help to promote the widespread adoption of Lithium-ion batteries in various applications.

REFERENCES

- [1] C. Z. El-bayeh, K. Alzaareer, A. I. Aldaoudyeh, B. Brahmi, and M. Zellagui, "Charging and Discharging Strategies of Electric Vehicles : A Survey," *WORLD Electr. Veh. J.*, pp. 1–29, 2021.
- [2] J. Wen, J. Jiang, and A. M. Function, "Battery Management System For the Charge Mode of Quickly Exchanging Battery Package," *IEEE Veh. Power Propuls. Conf.*, pp. 3–6, 2008.
- [3] I. Transactions and O. N. Instrumentation, "Measurement of the State of Battery Charge Using an Improved Loaded Voltmeter Test Method," *IEEE Trans. Instrum. Meas.*, vol. IM, no. 3, pp. 154–158, 1982.
- [4] A. R. Gade, "The New Battery Management System in Electric Vehicle," *Int. J. Eng. Res. Technol.*, vol. 10, no. 07, pp. 402–405, 2021.
- [5] B. Electric, V. Battery, and R. Engineering, "Analysis on Charging Safety and Optimization of Electric Vehicles," *2020 IEEE 6th Int. Conf. Comput. Commun. Anal.*, pp. 1–4, 2020.
- [6] M. Verasamy, M. Faisal, P. J. Ker, and M. A. Hannan, "Charging and Discharging Control of Li-Ion Battery Energy Management for Electric Vehicle Application," *Int. J. Eng. Technol.*, vol. 7, pp. 482–486, 2018.
- [7] H. Pierre-emmanuel, L. Liu, and G. Zhu, "State of Charge Estimation for Lion-Lithium Batteries Using Extended Kalman Theorem," *Int. Conf. Ind. Informatics-Computing Technol. Intell. Technol. Ind. Inf. Integr.*, pp. 295–298, 2015, doi: 10.1109/ICIIICIL.2015.154.
- [8] L. Rui-hao, S. Yu-kun, and J. Xiao-fu, "Battery State of Charge Estimation for Electric Vehicle Based on Neural Network," *IEEE*, pp. 193–196, 2011.
- [9] B. Bednar, L. Streit, and T. Kosan, "Diagnostic tool for Lithium and Lead-Acid Battery," *IEEE*, pp. 84–86, 2013.
- [10] R. Hasan and J. Scott, "Impedance Measurement of Batteries under load," *2019 IEEE Int. Instrum. Meas. Technol. Conf.*, pp. 1–5, 2019.
- [11] M. Grubmüller, B. Schweighofer, and H. Wegleiter, "Fast , High Accuracy , Freely Programmable Single Cell Battery Measurement System," *IEEE Instrum. Meas. Soc.*, vol. 1, 2015.
- [12] S. Gruber, M. Recheis, B. Schweighofer, and H. Wegleiter, "Low Distortion Power Amplifier for Battery Measurement Systems," *IEEE*, 2012.
- [13] Z. Haizhou, "Modeling of Lithium-ion Battery for Charging / Discharging Characteristics Based on Circuit Model," *Int. J. ONLINE Biomed. Eng.*, vol. 13, no. 06, pp. 86–95, 2017.
- [14] J. Olarte, J. Dauvergne, and A. Herrá, "Validation of thermal imaging as a tool for failure mode detection development," *AIMS Energy*, vol. 7, no. September, pp. 646–659, 2019, doi: 10.3934/energy.2019.5.646.
- [15] D. Bhattacharjee, P. Kalita, and S. B. Sarmah, "Investigation of Charging and Discharging Characteristics of Lithium-Ion Batteries for Application in Electric Vehicles Investigation of Charging and Discharging Characteristics of Lithium-Ion Batteries for Application," *Recent Res. Trends Energy Storage Devices*, no. January, pp. 43–54, 2021, doi: 10.1007/978-981-15-6394-2.